Supplement of Geochronology, 2, 101–118, 2020
https://doi.org/10.5194/gchron-2-101-2020-supplement

Supplement of

Extended-range luminescence dating of quartz and alkali feldspar from aeolian sediments in the eastern Mediterranean

Galina Faershtein et al.

Correspondence to: Galina Faershtein (galaf@gsi.gov.il)

Alkali-feldspar separation

The standard alkali-feldspar separation procedure includes two steps of heavy liquid separation at 2.62 and 2.58 gr cm^{-3} (Aitken et al., 1998) and is time consuming. In order to make the separation procedure more efficient, other separation methods were explored. Two samples from the Kerem Shalom (KR) section (KR-7, KR-9) were separated by three different methods: the standard two-step separation with heavy liquids (procedure A); magnetic separation through a LB-1 Frantz magnetic separator, using a current of 1.4 A on the magnet, followed by a one-step heavy liquid separation of the **nonmagnetic** fraction at 2.58 gr cm^{-3} (procedure B); or the **magnetic** fraction at the same density (procedure C). All the density-separated fractions lighter than 2.58 gr cm^{-3} were etched for 10 min with 10% HF solution (Porat et al., 2015) and measured with the pIR-IR_{290} protocol (Table 2 in the main text; average of 6 aliquots) and were analyzed with the Scanning electron microscope (SEM). and Ar

For both samples, the *De* values obtained from measuring aliquots separated with procedures A, B, and C are, within errors, similar (Table S1). SEM mapping showed that all the separated fractions are mostly composed of quartz, K-feldspar and Na-feldspar minerals with variable proportions (Fig. S1). Element mapping showed that for procedure B, the grains were mostly K-feldspar minerals (Fig. S1), almost identical to the grains separated with procedure A. On the other hand, there were significantly less K-feldspar mineral grains separated with procedure C. Therefore, procedure B, with one-step density separation at 2.58 gr cm^{-3} following magnetic separation, was selected for K-feldspar grains extraction. The heavy fraction of this separation can be farther used for quartz extraction.

Table S1: PIR-IR_{290} *De* values measured for samples KR-7 and KR-9 separated by the different procedures. N=6.

Sample	**Separation procedure**	***OD* (%)**	***De* (Gy)**
KR-7	A	17	168±29
	B	6	161±12
	C	1	196±7
KR-9	A	5	194±12
	B	10	224±27
	C	10	226±28

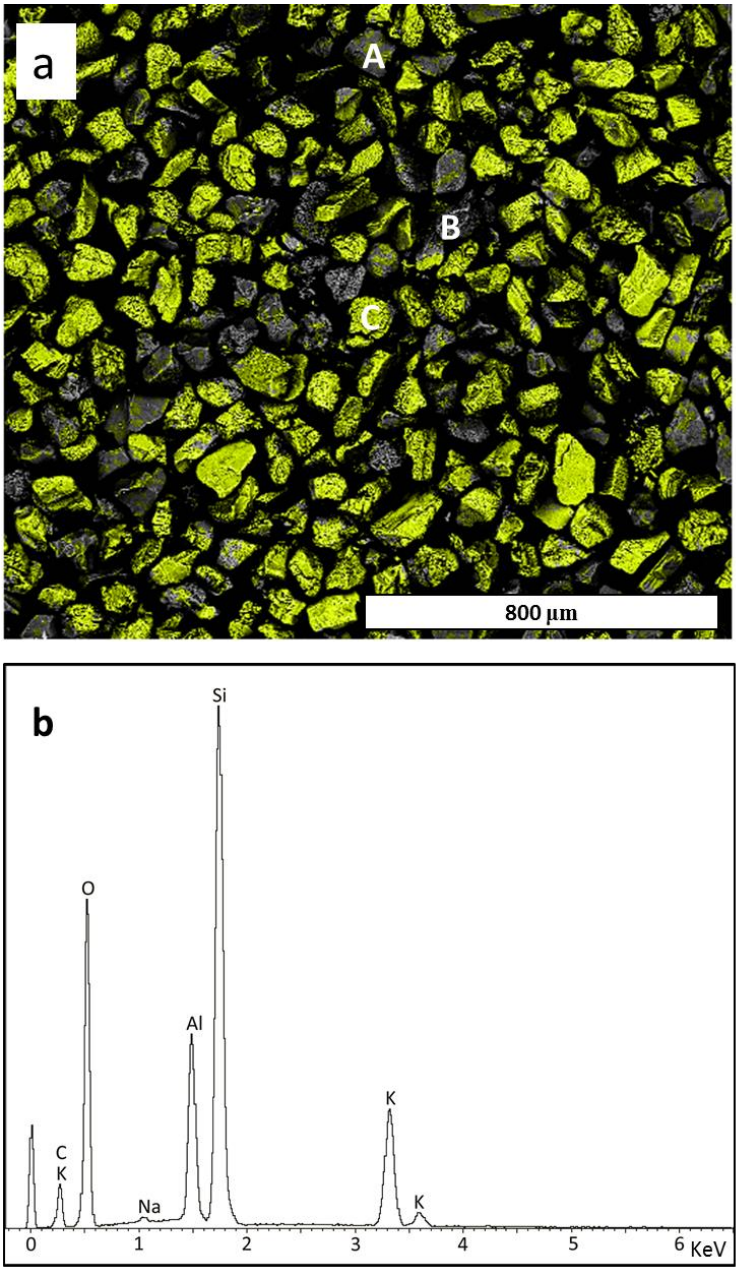

Figure S1: SEM results of sample KR-7 separated using procedure B. a) SEM image of the sample. Grains rich with potassium are colored in yellow. The sample contains Na-feldspar (A) quartz (B) K- feldspar (C – the majority of grains). B) SEM EDS composition spectra of mineral grain C indicating K-feldspar composition.

Table S2: Fading correction results of sample KR-1 following Kars et al. (2008) correction using the calc_Huntley2006 R function (King and Burow, 2019). The calc_Huntley2006 function was applied to all aliquots of samples KR-1, which were previously used for *De* determination. Then the function was applied using the average Ln/Tn value (with standard deviation) and a combined DRC of these aliquots. The average output parameters are almost identical (0-4% difference).

				Measured DRC				**Natural simulated DRC**			
Aliqout	***(n/N)*[a]**	***(n/N)*$_{ss}$[b]**		***De* [Gy]**	***D*$_0$ [Gy]**	**Age [ka]**		***De* [Gy]**	***D*$_0$ [Gy]**	**Age [ka]**	**2*D*$_0$ Age [ka]**
1	0.69±0.03	0.69±0.19		604±39	385±14	572±56		NaN	414±2	NaN	784±57
3	0.70±0.03	0.69±0.20		603±38	371±12	571±55		NaN	401±2	NaN	758±55
5	0.69±0.03	0.69±0.19		603±39	371±11	571±56		NaN	401±2	NaN	758±55
7	0.70±0.03	0.69±0.20		603±34	371±12	571±52		NaN	401±2	NaN	758±55
9	0.76±0.03	0.69±0.20		748±79	369±14	708±91		NaN	392±2	NaN	742±54
11	0.65±0.03	0.69±0.20		486±26	352±13	460±41		1137±177	382±1	1076±185	724±53
13	0.79±0.03	0.69±0.19		779±82	340±13	737±94		NaN	359±2	NaN	679±50
15	0.70±0.03	0.69±0.20		545±36	330±11	515±51		NaN	355±2	NaN	672±49
Average	0.71±0.04	0.69±0.00		621±97	361±19	588±92		NaN	388±21	NaN	734±40
Combined	0.71±0.07	0.69±0.19		595±177	348±4	563±172		NaN	378±2	NaN	715±52

[a] The level of saturation.

[b] The field saturation.

Table S3: Details of additional samples used in the study for various experiments. All samples are of aeolian sediments originated from the Nile.

Sample	**site**	**Mineral**	**Grain size (μm)**	**Source**	**Remarks**
DF-13	Negev Dune field	quartz	150-177	Roskin et al., 2011	OSL age 40±10 years
ML-D-13	Shefayim	feldspar	150-177	Geological Survey of Israel (GSI) luminescence laboratory unpublished data	Modern beach sample
RUH-40	Ruhama	quartz	90-125	GSI luminescence laboratory unpublished data	TT-OSL *De* 42±2 Gy
RUH-90	Ruhama	quartz	90-125	GSI luminescence laboratory unpublished data	TT-OSL *De* 53±3 Gy
RUH-180	Ruhama	quartz	90-125	GSI luminescence laboratory unpublished data	TT-OSL *De* 163±15 Gy
RUH-300	Ruhama	quartz	90-125	GSI luminescence laboratory unpublished data	TT-OSL *De* 264±11 Gy

Table S4: Fading data for Kerem Shalom samples. For each sample the *g*-value and ρ' of 3 aliquots and averages are presented. Samples KR-11 to KR-15 were not measured for fading.

Sample	**Depth [m]**	***g*-value (% per decade)**	**Average *g*-value (% per decade)**	**ρ' (*10^{-6})**	**Average ρ' (*10^{-6})**
KR-17	0.5	0.7±0.53	1.43±0.63	0.71±0.55	1.50±0.69
		1.84±0.51		1.95±0.54	
		1.75±0.51		1.85±0.54	
KR-6	1.5	1.42±0.51	1.47±0.18	1.50±0.53	1.55±0.20
		1.67±0.50		1.77±0.53	
		1.32±0.50		1.39±0.54	
KR-16	1.5	1.51±0.51	1.24±0.44	1.59±0.54	1.14±0.57
		0.73±052		0.74±0.54	
		1.48±0.51		1.54±0.54	
KR-7	2.3	2.75±0.53	1.49±1.09	2.92±0.57	1.58±1.16
		0.9±0.56		0.94±0.59	
		0.82±0.55		0.87±0.57	
KR-8	3	1.06±0.54	1.35±0.28	1.11±0.58	1.41±0.28
		1.38±0.54		1.44±0.58	
		1.61±0.55		1.67±0.58	
KR-5	4.1	1.44±0.50	1.21±0.20	1.52±0.53	1.28±0.21
		1.11±0.49		1.17±0.53	
		1.08±0.49		1.14±0.52	
KR-9	4.1	0.96±0.58	1.54±0.84	1.02±0.61	1.64±0.89
		1.16±0.58		1.25±0.60	
		2.5±0.56		2.66±0.61	
KR-10	5.2	1.52±0.58	1.63±0.28	1.61±0.62	1.70±0.34
		1.95±0.57		2.07±0.56	
		1.42±0.58		1.41±0.61	
KR-3	10.7	1.71±0.48	1.66±0.28	1.82±0.51	1.76±0.30
		1.36±0.48		1.43±0.51	
		1.91±0.52		2.03±0.56	
KR-2	12.5	1.4±0.6	1.20±0.18	1.47±0.64	1.26±0.19
		1.08±0.56		1.13±0.60	
		1.11±0.52		1.17±0.55	
KR-1	15.3	0.92±0.78	1.17±0.36	1.00±0.46	1.32±0.38
		1.01±1.05		1.23±0.94	
		1.58±0.46		1.74±0.52	

Table S5: VSL MAAD ages. The *Ln/Tn* values of the KR samples were projected onto the MAAD DRC constructed for the modern quartz sample DF-13 fitted with one exponential plus linear and two exponentials function.

				One exponential plus lineal function		**Two exponentials function**	
Sample	**Depth (m)**	**Dose rate (Gy kyr^{-1})**	***Ln/Tn***	***De* (Gy)**	**Age (ka)**	***De* (Gy)**	**Age (ka)**
KR-6	1.5	1.22±0.07	0.22±0.09	29±18	24±14	24^{+43}_{-10}	20^{+35}_{-8}
KR-16	1.5	1.20±0.06	0.15±0.02	17±3	14±3	13^{+17}_{-10}	11^{+14}_{-9}
KR-7	2.3	1.60±0.08	0.29±0.05	45±12	28±8	40^{+53}_{-29}	25^{+33}_{-18}
KR-8	3	1.56±0.08	0.42±0.02	87±8	56±5	85^{+96}_{-76}	55^{+62}_{-49}
KR-5	4.1	1.32±0.07	0.46±0.05	108±29	82±22	113^{+161}_{-82}	85^{+122}_{-62}
KR-9	4.1	1.23±0.07	0.48±0.07	121±51	98±42	131^{+221}_{-83}	106^{+179}_{-67}
KR-10	5.2	1.36±0.07	0.57±0.07	227±175	166±128	265^{+449}_{-155}	194^{+329}_{-114}
KR-11	5.8	1.54±0.08	0.69±0.10	785±514	510±334	726^{+6215}_{-320}	472^{+4041}_{-208}
KR-4	6.3	1.56±0.08	0.49±0.07	130±57	83±37	144^{+243}_{-90}	92^{+156}_{-58}
KR-12	7.2	1.70±0.09	0.61±0.08	352±296	208±174	361^{+693}_{-196}	213^{+408}_{-115}
KR-13	8.2	1.01±0.05	0.64±0.05	508±240	501±237	462^{+705}_{-317}	456^{+696}_{-313}
KR-14	9.5	1.27±0.05	0.72±0.07	954±370	749±291	1094^{+6064}_{-518}	860^{+4763}_{-407}
KR-3	10.7	1.05±0.06	0.51±0.09	149±133	141±126	170^{+362}_{-87}	162^{+344}_{-82}
KR-15	11.7	0.73±0.04	0.70±0.10	826±526	1131±720	788^{+6256}_{-337}	1080^{+8570}_{-462}
KR-2	12.5	0.68±0.04	0.63±0.13	458±511	674±751	429^{+6208}_{-155}	631^{+9130}_{-229}
KR-1	15.3	0.68±0.05	0.70±0.05	815±260	1200±382	773^{+5256}_{-498}	1137^{+7730}_{-732}
DF-13			0.02±0.01				

References:

Aitken, M.J.: An Introduction to Optical Dating: the Dating of Quaternary Sediments by the Use of Photon-stimulated Luminescence. Oxford University Press,1998.

Kars, R.H., Wallinga, J., Cohen, K.M.: A new approach towards anomalous fading correction for feldspar IRSL dating — tests on samples in field saturation. Radiation Measurements 43, 786–790, 2008.

King, G.E., Burow, C.: calc_Huntley2006(): Apply the Huntley (2006) model. Function version 0.4.1. In: Kreutzer, S., Burow, C., Dietze, M., Fuchs, M.C., Schmidt, C., Fischer, M., Friedrich, J.: Luminescence: Comprehensive Luminescence Dating Data AnalysisR package version 0.9.5. https://CRAN.R-project.org/package=Luminescence, 2019.

Porat, N., Faershtein, G., Medialdea, A., Murray, A.S.: Re-examination of common extraction and purification methods of quartz and feldspar for luminescence dating. Ancient TL 33, 22-30, 2015.

Roskin, J., Porat, N., Tsoar, H., Blumberg, D.G., Zander, A.M.: Age, origin and climatic controls on vegetated linear dunes in the northwestern Negev Desert (Israel). Quaternary Science Reviews 30, 1649-1674, 2011.